ChemComm

FEATURE ARTICLE

View Article Online
View Journal | View Issue

Cite this: *Chem. Commun.*, 2022, **58**, 5332

Selective coordination of coinage metals using orthogonal ligand scaffolds

Vanitha R. Naina,† Frederic Krätschmer† and Peter W. Roesky *

Received 22nd February 2022,
Accepted 4th April 2022

DOI: 10.1039/d2cc01093c

rsc.li/chemcomm

Group 11 metal complexes with their ability to form metallophilic interations are widely pursued to develop multifunctional luminescent materials. Heteronuclear coinage metal complexes are promising candidates to tune electronic and optical properties which are not readily accessed by their homometallic congeners. In this review, we present the concept of orthogonal ligands which are rationally designed to access heteronuclear coinage metal complexes and studied in terms of their photophysical properties. Bifunctional ligands containing soft and hard donor atoms have the potential of providing different coordination modes to selectively synthesise heterobimetallic complexes in a predictable manner. This review deals with ligand sets composed of pyridine, bipyridine- or iminopyridine-substituted NHCs featuring C–N coordination modes, phosphine-based N-heterocycles and amidinate ligand scaffolds comprising of P–N functionalities and mixed phosphine–phosphine oxide with P–O donor sites. Therefore, the scope of this perspective is the discussion of heteronuclear coinage metal complexes supported by recently developed bifunctional ligands in terms of their synthesis, coordination geometries and tunability of optical properties when compared to their homometallic analogues.

Introduction

Light harvesting devices such as OLEDs or solar cells have attracted great attention as they are promising means to harness renewable energy sources (solar energy).[1] Coinage metal complexes have found potential applications in the field of organic photovoltaics owing to their remarkable optical properties. Group 11 metals in +1 oxidation state are known for their ability to form d^{10}–d^{10} interactions termed as ''metallophilicity''.[1–6] For gold, these ''aurophilic interactions''[4,5] arise only when the distance between two metal atoms falls below 3.5 Å *i.e.* less than the sum of the van der Waals radii of two gold atoms. Although less known, these interactions were also observed for coinage congeners (Cu and Ag) with closed shell electronic configuration. They are referred as ''cuprophilic'' with distance between Cu(I) cations below 2.8 Å[7,8] and ''argentophilic'' interactions when the distance between two silver(I) cations is in the range of 2.9–3.4 Å.[6,9,10] In principle, these bonds are supported by a number of ligands, hence, can be modulated by fine tuning of the ligand backbone,[11] solvents[12] *etc.* These interactions not only play a crucial role in stabilising supramolecular structures but also in determining the optical properties of the metal complexes.[13–16] A critical review on homometallic and heterometallic clusters involving these weak d^{10}–d^{10} attractive interactions was published by Braunstein and co-workers in 2011.[17]

A wealth of literature is available on coinage metal complexes with interesting properties such as thermochromism, vapochromism, *etc.*[12,18–23] Structurally well-characterised heterometallic assemblies have been widely investigated in order to establish structure–property correlations and to pursue multifunctional light-emitting materials. The presence of different metal ions in a molecular architecture often leads to distinct properties (due to synergistic effects) when compared to their analogues of monometallic combinations.[13,24] This review is intended to be of tutorial nature wherein, we particularly focus on a selective set of rationally designed orthogonal ligands which allow the synthesis of multimetallic complexes, in which the metals are arranged in defined compartments showing supported metallophilic interactions in many cases. These compounds were systematically studied with respect to their photoluminescence properties.

Multiple comprehensive reviews focusing on the properties of polynuclear coinage metal complexes have been reported.[25–27] Recently, Koshevoy, Grachova and co-workers published a review devoted to optical properties of multinuclear coinage metal complexes based on bridging phosphine ligands.[28] Even though, phosphines have affinity for all the group 11 metals with d^{10}-electronic configuration and often result in fascinating properties,[29,30] it is difficult to selectively design heterometallic

Institute of Inorganic Chemistry, Karlsruhe Institute of Technology, Engesserstr. 15, 76131 Karlsruhe, Germany. E-mail: roesky@kit.edu
† These authors contributed equally to this work.

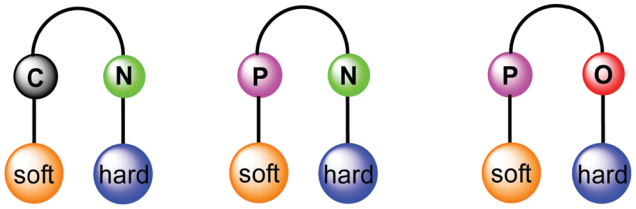

Fig. 1 Schematic representation of orthogonal ligand scaffolds with selective coordination to metal ions following the HSAB principle.

complexes due to the scrambling nature of metal ions between different phosphorous donor sites in solution state.[31] Hence, it is of no doubt that the synthesis of stable heterometallic complexes demand a rational ligand engineering, which can selectively coordinate to different metal ions. In group 11 chemistry, the formation of heterometallic complexes has been used for the synthesis of luminescent materials. However, the challenge is the selective assembly of such compounds.

Orthogonal ligands, commonly referred as bifunctional ligands, can be defined as organic ligands containing two different coordinating sites, which can selectively coordinate to two different metal ions. From conventional Pearson concept of hard and soft acid and bases (HSAB),[32,33] in group 11 Au(I) prefers coordinating to soft donors (*e.g.*, P) in comparison to hard donors (*e.g.*, N, O), whereas Cu(I) has a greater affinity for the hard donor atoms and Ag(I) is somewhere in between. Following this principle, ligands having several heteroatoms as coordination sites are suitable for the selective construction of heterometallic architectures in order to tune the properties of interest. Moreover, multidentate ligands allow several combinations (Fig. 1) and spatial proximity of different metal ions leading to metal–metal interactions. This point of view has led to the development of ligands with tailor-made steric and electronic properties. Earliest example of orthogonal ligand based heteronuclear complex was reported by Che and co-workers in 1998.[34] Having emphasised the principal role of multidentate ligands with heteroatoms, it is noteworthy that there are other ways to achieve the focused goal *e.g.*, introducing coordinating anions like CN-,[35,36] triflate,[37] or solvents such as acetonitrile and pyridine.[38–40]

Herein, we particularly intend to discuss a limited set of ligands, which are reported in the past few years. This review has been categorised into three sub-groups based on the coordination modes present in the ligand namely C–N, P–N, P–O.

C–N coordination

Coordination modes

Complexes of the coinage metals with N- and C-donor ligands are embossed by tetrahedral, trigonal planar and linear coordination modes. To investigate on this behaviour, a series of ligands with rather soft carbene donor functionalities for gold(I) atoms and a tethered pyridine, bipyridine or iminopyridine moiety as hard donor for copper(I) and silver(I) atoms ($\mathbf{L^1}$–$\mathbf{L^6}$) were used (Schemes 1, 2, 4, 6, and 7).[20,22,41–46] In case of gold(I), linear coordination with soft carbene donor functionalities was obtained for all compounds shown in Schemes 1, 2, 4, 6, and 7.

By using Ag_2O for deprotonation of $\mathbf{L^1}$ followed by transmetallation with a gold(I) salt, the monometallic gold(I) compound **1** was synthesised (Scheme 1). Treatment of **1** with silver(I) or copper(I) salts resulted in the formation of heterobimetallic compounds **2** and **3** (Scheme 1 (right)).[41] The coordination of gold(I) to the bipyridine moiety was not observed, as expected for a soft metal. Starting with $\mathbf{L^1}$, the homobimetallic silver(I) complex **4** was obtained from the corresponding silver(I) precursors, while compound **5** was synthesised by transmetallation of an *in situ* generated silver(I) species with a copper(I) salt (Scheme 1 (left)).[41] Copper(I) and silver(I) prefer the hard N-donor functionalities. Nevertheless, in the absence of gold(I) also coordination to soft donors concomitant with the formation of homometallic complexes is possible. Copper(I) is most often tetrahedrally coordinated but can also form trigonal planar or linear arrangements (Schemes 1, 2, 4, 5, and 7).

The propensity of silver(I) to adopt low coordination numbers and a linear coordination is reflected by the almost linear arrangement of N–Ag–N′ ($> 160^\circ$) in the bipyridine units (**3**). In addition, there is a higher tendency of silver(I) to form metallophilic contacts, which is reflected by the smaller intermetallic distance Ag–Ag (3.1034(11) Å) (**5**) compared to the copper(I) homologue (3.2168(9) Å) (**4**) despite the larger van der Waals radius (Scheme 1 and Fig. 2).[41]

With the intention of synthesising tetranuclear coinage metal chains the bis-NHC^{bipy} ligand $\mathbf{L^2}$, composed out of two $\mathbf{L^1}$ moieties, was designed.[42] The synthesis of the coinage metal complexes **6–8** (Scheme 2) was achieved in a similar fashion to compounds **1–3**.[41] While the homobimetallic gold(I) compound **6** does not show intermetallic interactions, the coordination of copper(I) atoms into the bipyridine moieties in compound **7** leads to a V-shaped structure with a shorter Au–Au distance of 3.38 Å and Au–Cu distances of around 4.95 Å (Scheme 3). In contrast silver(I) complex **8**, which is ligated by $\mathbf{L^2}$, shows two

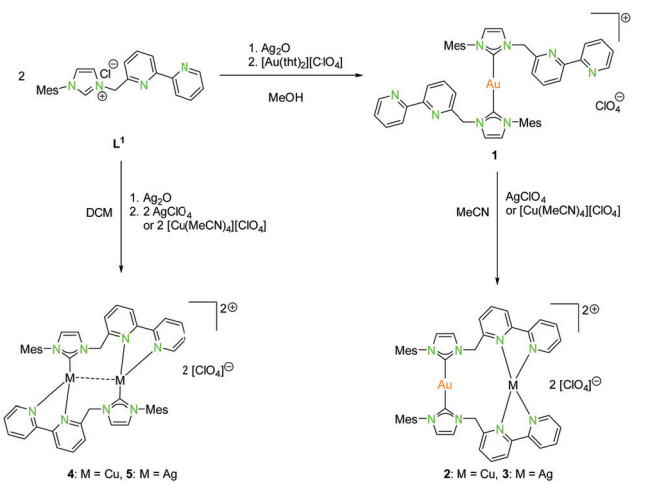

Scheme 1 Synthesis of mononuclear (**1**), dinuclear homo- (**4**, **5**) and heterobimetallic (**2**, **3**) compounds with NHC^{bipy} ($\mathbf{L^1}$).[41]

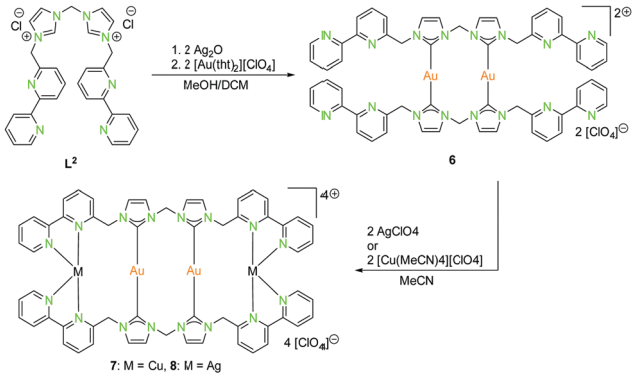

Scheme 2 Synthesis of homometallic dinuclear (**6**) and heterometallic tetranuclear (**7**, **8**) bis-NHC^{bipy} (**L^2**) compounds.[42]

Scheme 3 V-shaped (left) and zig-zag chain (right) structures of compound **8**.[42]

molecules in the asymmetric unit, one homologue to the V-shaped copper(I) compound **7** without metallophilic interactions (Au–Au 3.80 Å, Au–Ag *ca.* 5.16 Å), and a zig-zag chain structure with metallophilic interactions between all neighbouring atoms (Au–Au 3.05 Å, Au–Ag *ca.* 2.97 Å) (Scheme 3). This structural arrangement can only be achieved by a folding of the ligand.[42]

A rather similar ligand to **L^1** is the NHC^{impy} system **L^3**, in which the bipyridine moiety was exchanged by an iminopyridin scaffold (Scheme 4).[43] The synthesis of the coinage metal complexes ligated to **L^3** is shown in Scheme 4. They were obtained in a similar synthetic approach as used for the synthesis of the compounds discussed above. Only the homobimetallic copper(I) compound **12** was synthesised differently

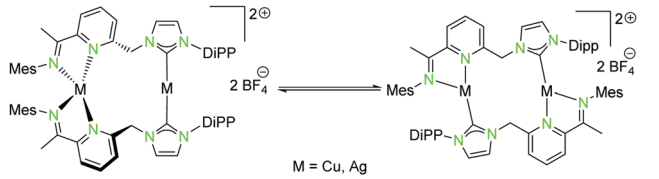

Scheme 5 Isomerisation of homometallic NHC^{impy} (**L^3**) compounds (**12**, **14**) in solution.[43]

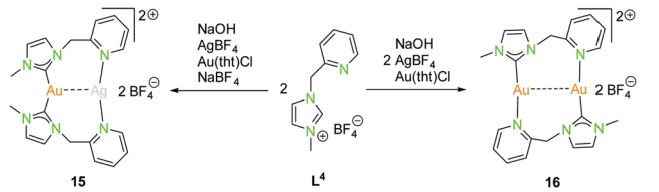

Scheme 6 Synthesis of heterometallic dinuclear (**15**) and homometallic dinuclear (**16**) NHC^{py} (**L^4**) compounds.[47]

by deprotonation of **L^3** with mesityl copper(I) followed by halide abstraction with $AgBF_4$.[43]

The solid state structure of the homometallic silver(I) iminopyridine complex **14** shows a distorted trigonal planar coordination ("head to tail"), whereas for the copper(I) compound **12** a linear and a tetrahedral distorted coordination ("head to head") was found. Nevertheless, these two compounds isomerise in solution and thus form both coordination modes (Scheme 5).

The heterobimetallic compounds **10** and **11** show "head to head" arrangement, which is in contrast to the homobimetallic silver(I) complex **14** probably due to the formation of stronger Au–NHC bonds and the aversion of gold(I) to hard donor sites.[43] Like the homobimetallic compounds **12** and **14**, the heterobimetallic compounds show no metallophilic interactions with intermetallic distances largely exceeding the van der Waals radii (Au–Cu 4.91 Å, Au–Ag 5.14 Å).[43]

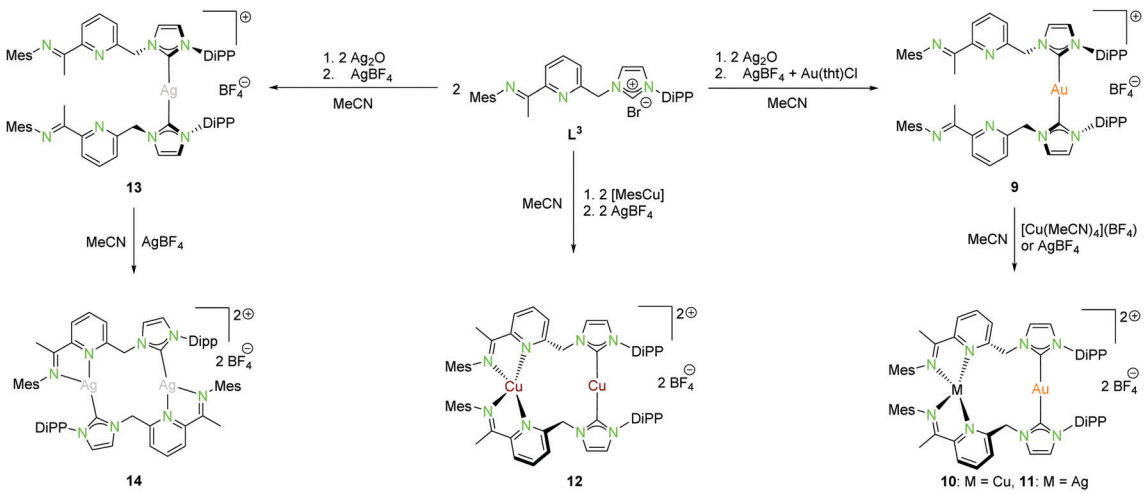

Scheme 4 Synthesis of mononuclear (**9**, **13**), as well as homo- (**12**, **14**) and heterobimetallic (**10**, **11**) NHC^{impy} (**L^3**) compounds.[43]

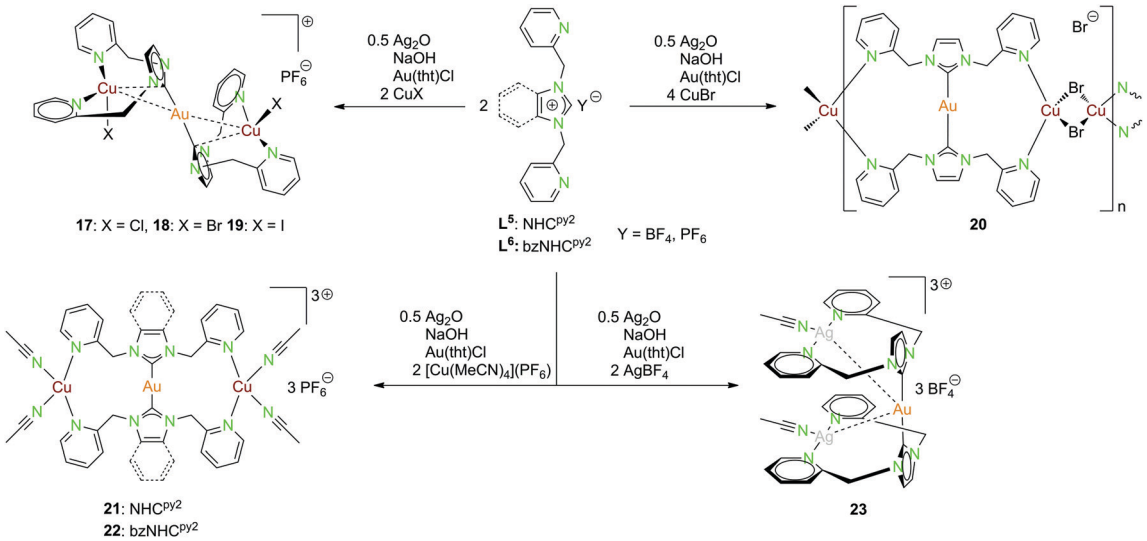

Scheme 7 Synthesis of the heterotrinuclear complexes **17–23** with NHC^{py2} ($\mathbf{L^5}$) and $bzNHC^{py2}$ ($\mathbf{L^6}$).[20,22,45,46]

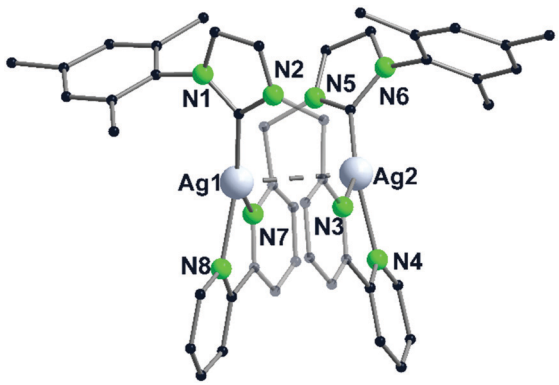

Fig. 2 Molecular structure of **5** in the solid state. Hydrogen atoms and the counter ions are omitted for clarity.[41]

The following compounds from Catalano *et al.* are quite similar NHC ligands, but instead of an attached bipyridine functionality, which is favourable for tetrahedral coordination, pyridine units are used.[20,22,45–47] This results in different coordination modes and leaves space for coordinating solvent molecules.

The dinuclear NHC^{py} ($\mathbf{L^4}$) complexes **15** and **16** can be synthesised by deprotonation through NaOH, addition of $AgBF_4$ leads to $[(NHC^{py})_2Ag][BF_4]$ and is transferred to $[(NHC^{py})_2Au][BF_4]$ using Au(tht)Cl, followed by the addition of $AgBF_4$ or *in situ* synthesised $Au(tht)BF_4$ (Scheme 6).[47]

The heterometallic gold(I)–silver(I) complex **15** is arranged in a "head to head" fashion, where gold(I) is coordinated in a distorted linear geometry by two NHC's and silver(I) is coordinated to two pyridyl moieties, not considering the metallophilic interaction (Au–Ag 3.03 Å).[47] The C–Au–C angle is 170.6°, which is more linear than the N–Ag–N angle of 154.6°. The homometallic gold(I) compound **16** is in a "head to tail" fashion with gold(I) coordinated to one NHC and a pyridyl moiety in a nearly linear manner.[47] The "head to head" coordination is inconvenient due to the fact, that one gold atom would be coordinated by two hard nitrogen donors which is in contradiction to the HSAB principle. The bond angles C–Au–N are close to 180° (179.4° and 178.5°). The intermetallic distance (Au–Au 3.17 Å) is slightly longer than in the heteronuclear compound **15** (Au–Ag 3.03 Å).[47]

Multiple heterometallic gold(I)–copper(I) halide compounds (**17–20**) were synthesised using the NHC^{py2} ligand ($\mathbf{L^5}$).[46] The ligand was deprotonated by NaOH and Ag_2O, with transmetallation to the $[(NHC^{py2})_2Au](PF_6)$ complex using Au(tht)Cl and followed by addition of copper(I)–halides (Scheme 7).[46]

Compounds **17–19** are isostructural, with gold(I) being nearly linear coordinated by the two ligand moieties. Each copper(I) is coordinated by two pyridyl functionalities of the same ligand, as well as one halide and a short contact to the NHC carbon. The gold(I)–copper(I) separations range from 2.6688(9) Å in **18** over 2.6786(10) Å in **19** to 2.7030(5) Å in **17** (Fig. 3).[46]

Compound **20** forming a polymeric structure shows an almost linear coordinated gold(I) centre but unlike the previous compounds the two copper(I) centers coordinate to two pyridyl units at opposed ligands. The distorted tetrahedral coordination sphere is completed by two bridging bromide ions. No intermetallic interactions occur for this compound.[46] The trinuclear heterometallic compounds **21** and **22** can be isolated when reacting the ligands NHC^{py2} ($\mathbf{L^5}$) and $bzNHC^{py2}$ ($\mathbf{L^6}$) with $[Cu(MeCN)_4](PF_6)$ instead of copper(I) halides (Scheme 7).[20,22]

Gold(I) is nearly linear coordinated by two carbon atoms, while the two copper(I) centers are coordinated by two pyridyl functionalities and two acetonitrile molecules in a distorted tetrahedral geometry. The Au–Cu separation is in both cases around 4.6 Å, the replacement of acetonitrile by one methanol (**21**) or the complete abstraction (**22**) leads to considerably shorter intermetallic contacts (2.8 Å, 3.0 Å).[20,22]

The gold(I)–silver(I) trinuclear compound **23** was synthesised using NHC^{py2} ($\mathbf{L^5}$), following the pathway mentioned above,

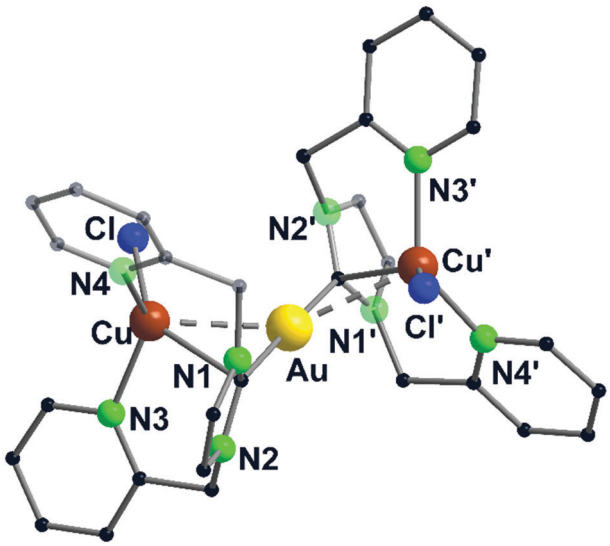

Fig. 3 Molecular structure of **17** in the solid state. Hydrogen atoms and the counter ions are omitted for clarity.[46]

with the addition of two equivalents $AgBF_4$ in the last step (Scheme 7).[45] The gold(I) centre is coordinated by the two NHC carbon atoms. Like in compound **17–19**, silver(I) is coordinated by the pyridyl units of the same ligand and one acetonitrile molecule in a T-shaped geometry. Therefore, the pyridine rings are splayed back, achieving an almost orthogonal position to the imidazole ring.[45] The intermetallic distances between gold(I) and silver(I) are about 3.25 Å and the silver(I)–silver(I) distance is 3.43 Å close to argentophilic interactions (Fig. 4).[45]

All mentioned complexes follow the HSAB principle, showing the coordination of gold(I) with low coordination numbers and almost exclusively soft donor sites. Copper(I) mostly shows tetrahedral coordination or in rare cases a coordination between linear and tetrahedral arrangement always looking for high coordination numbers with hard donors. In the case of silver(I), it can be emphasised that it lies in between, wanting low coordination numbers but coordinates to hard as well as soft donors.

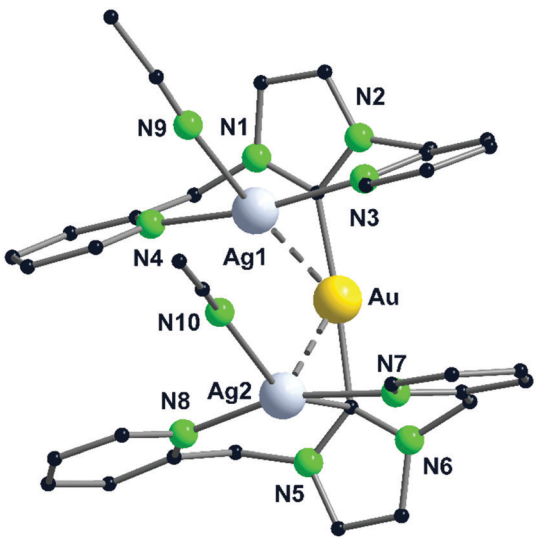

Fig. 4 Molecular structure of **23** in the solid state. Hydrogen atoms and the counter ions are omitted for clarity.[45]

Photoluminescence properties

For compounds **1–14** shown above (Schemes 1, 2 and 4), a vibronically structured greenish PL emission around 480 nm is observed. The exceptions are the mononuclear gold(I) compound **9**, the homobimetallic copper(I) complex **4** and the gold(I)–copper(I) heterobimetallic complexes (**2**, **7** and **10**), where the presence of the copper(I) leads to a broad band at higher wavelengths. This already indicates a strong influence of the copper(I) ion in heterobimetallic complexes to their PL properties. The spectra of compounds **1–8**, which contain one of the NHC^{bipy} ligands ($\mathbf{L^1}$ or $\mathbf{L^2}$) resemble each other (Fig. 5 and 6),[41,42] since ligand $\mathbf{L^2}$ is formally built from two of the coordinating units of $\mathbf{L^1}$. The vibronic structures in the spectra of these compounds were assigned to intraligand (IL) transition centered on the bipyridine moieties.

The PLE onset at around 400–440 nm is consistent with the colourless and yellowish colour of the compounds, but in discrepancy with the orange to brown copper(I) containing compounds. The contributions from the d-orbitals of copper(I) lead to a significant decrease of the HOMO–LUMO gap, resulting in the redshift of absorption.[41,42] This was explained by TDDFT calculations by using the trinuclear di(bipyridine)phenylphosphine ligated Cu–Au–Cu complex **32** as model compound

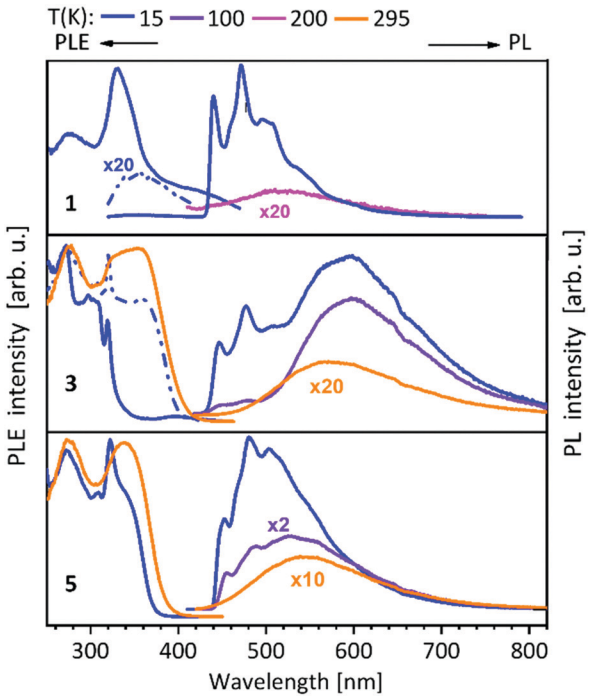

Fig. 5 Solid state excitation and emission spectra of NHC^{bipy} ($\mathbf{L^1}$) metal complexes **1**, **3**, **5**. PL was excited at λ_{exc} = 300 nm and PLE spectra were recorded at λ_{em} = 540/540 nm (**1**), λ_{em} = 480; 580/580 nm (**3**) and λ_{em} = 550/550 nm (**5**).[41]

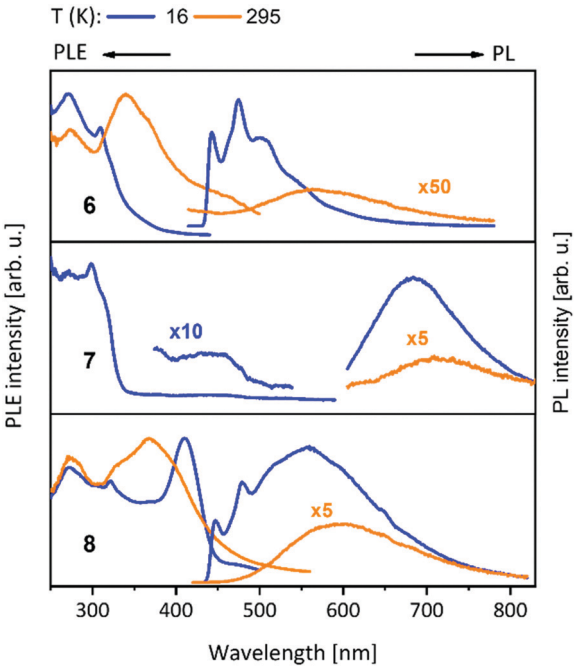

Fig. 6 Solid state excitation and emission spectra of bis-NHC^{bipy} ($\mathbf{L^2}$) metal complexes **6–8**. PL was excited at λ_{exc} = 300 nm for **6**, **8** and λ_{exc} = 320 nm for **7**. PLE spectra were recorded at λ_{em} = 500/560 nm (**6**), λ_{em} = 700/750 nm (**7**) and λ_{em} = 550/600 nm (**8**) at low/elevated temperatures respectively.[42]

(see below and Scheme 10).[48] Also, the participation of copper(I) with photoexcitation into lower-energy excited states results in very efficient non-radiative relaxation. In contrast, the contribution by silver(I) and gold(I) atoms occurs at comparably low energies, thus these orbitals do not play a role for the excitations and have no significant influence on the optical properties.[49] The PL spectra of the $\mathbf{L^3}$ ligated complexes (**9–14**) (Fig. 7) resemble the ones discussed above (compounds **1–8**) (Fig. 5 and 6).[41,43]

The PL properties of compounds **1–14** can be finely tuned by the loaded metal, in particular the structural homologue AuCu and AuAg complexes demonstrate different emission spectra. Moreover, the PL efficiency depends on the ligand framework.

In this case $\mathbf{L^3}$ coordinated compounds show a much weaker emission,[43] especially at lower temperatures, than $\mathbf{L^1}$ ligated compounds.[41] The structural flexibility of the imino-pyridine function may lead to efficient non-radiative relaxation and PL quenching.[43]

Compounds **15–23** (Table 1) having closely related ligands ($\mathbf{L^4}$–$\mathbf{L^6}$) (Schemes 6 and 7) show no vibronic structure in their spectra.[20,22,45–47] The NHC^{py} ($\mathbf{L^4}$) compound **15** bearing gold(I) and silver(I) shows a sharp band at 416 nm. Exchange of silver(I) by gold(I) in **16** leads to a small shift to 423 nm at 77 K. At room temperature, a broad band at 475 nm can be seen for compound **16**.[47] NHC^{py2} ($\mathbf{L^5}$) compounds **17–19** show similar spectra with the band maximum shifted following the Au(I)–Cu(I) separation (Br < I < Cl) with the shortest distances having the highest energy band (509 nm in **18**, 514 nm in **19** and 517 nm in **17** at 77 K). The polymeric bromine compound **20** exhibits red shifted emission at 533 nm.[46] The almost identical compounds **21** ($\mathbf{L^5}$) and **22** (bzNHC^{py2} ($\mathbf{L^6}$)) feature identical narrow emission bands at 461 nm (**21**) and 462 nm (**22**).[20,22] The trinuclear complex **23** exhibits strong bright blue luminescence at 455 nm, with enhanced intensity of the emission band when compared to the mononuclear gold(I) precursor [(NHC^{py2})$_2$Au][BF$_4$].[45]

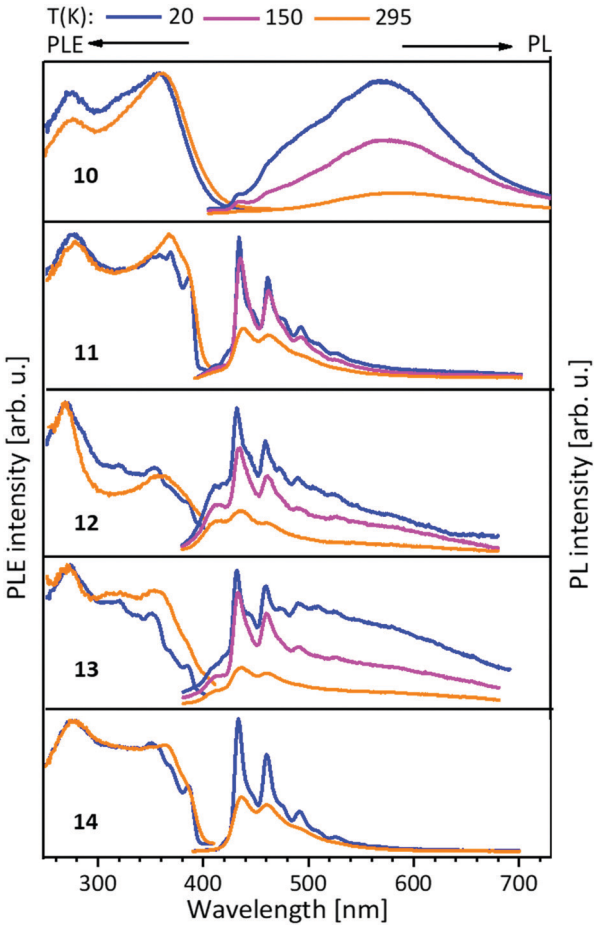

Fig. 7 Solid state excitation and emission spectra of NHC^{impy} ($\mathbf{L^3}$) metal complexes **10–14**. PL was excited at λ_{exc} = 350 nm and PLE spectra recorded at λ_{em} = 580 nm for **10** and λ_{em} = 430 nm for **11–14**, λ_{em} = 430/460 nm (**13**).[43]

The PL data of compounds **15–23** indicate a clear trend in the energy of the emission peaks by changing the metal loading. Gold(I), silver(I) containing compounds experience a hypsochromic shift, while copper(I) containing compounds are red shifted. Also, the importance of metallophilic interaction on the PL properties can be shown nicely by compounds **17–19** (Table 1).

P–N coordination

Coordination modes

Another approach for ligand systems, capable of multidentate coordination with soft as well as hard donor functionalities, can be achieved by combining phosphorus and nitrogen donor sites. Despite the number of other P–N ligand systems,[13,50–53]

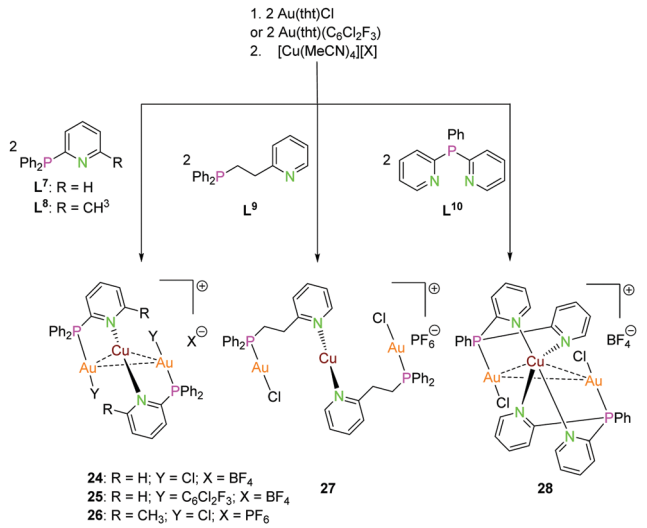

Scheme 8 Synthesis of trinuclear heterometallic P^{py} (L^7–L^{10}) compounds **24–28**.[13,51,54]

we focused on papers in which correlation with luminescence properties are considered. Gimeno and co-workers have used bifunctional phosphine ligands (L^7, L^9 and L^{10}) with pyridine in the backbone in 2010 to access heteronuclear complexes **24**, **27** and **28**. On reacting the mononuclear gold(I) complexes with $[Cu(MeCN)_4](X)$ (X = BF_4 or PF_6) in 2 : 1 molar ratio led to the isolation of trinuclear complexes depicted in Scheme 8.[13] The molecular structure of complex **24** in the solid state is established by X-ray analysis revealing a Au_2Cu core supported by two ligand scaffolds with an aurophilic (Au1–Au2) interactions of 3.0658(5) Å and Au–Cu contacts in the range of 2.98–3.05 Å.[13] Catalano and co-workers synthesised compound **25** with gold(I) coordinated by $C_6Cl_2F_3$, with parameters similar to those of the closely related chloride compound **24**.[54]

Au(I) ions are coordinated to a phosphine group and the charge on the ion is balanced by the coordinating chloride. As expected, copper(I) is bonded to the nitrogen atoms of the pyridine moieties. Au(I) and Cu(I) adapt almost linear geometry.[13] Complex **27** is also proposed to have a Au_2Cu core supported by two ligand scaffolds due to its orange colour which can be ascribed to metallophilic interactions. It is likely that the copper(I) ion is coordinated to four nitrogen atoms thereby resulting in tetrahedral geometry which is different from **24**.[13] Complex **27** is also comprised of two ligand units and the metal ions defining similar coordination as **24**.[13] However, in compound **27**, the long alkyl linker between pyridine and phosphine groups inhibits metal–metal interactions to exist.

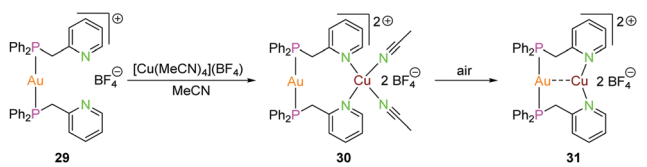

Scheme 9 Synthesis of dinuclear heterometallic compounds **29–31** with P^{py} ligand (L^{11}).[55]

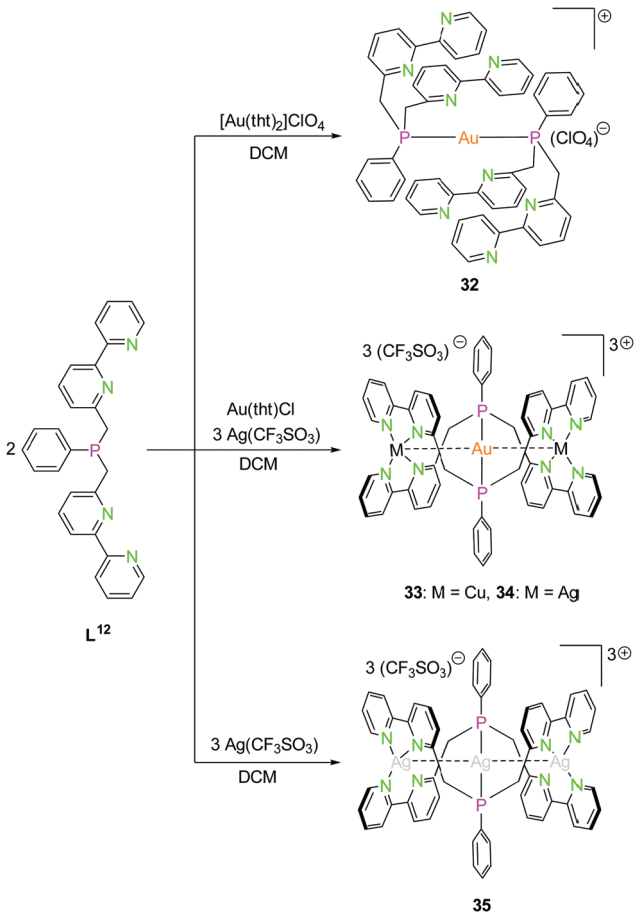

Scheme 10 Synthesis of mononuclear gold(I) (**32**) and trinuclear hetero- (**33**, **34**) and homometallic silver(I) (**35**) PN_4 (L^{12}) compounds.[48]

The proposed coordination modes in complex **27** and **28** are supported by ^1H and $^{31}P\{^1H\}$ NMR experiments.[13] Hobbollahi *et al.*, reported a tri-nuclear complex **26** with L^8 and Au_2Cu core in 2017 with similar bonding modes to that of **24** which exhibits cold-white emission (Scheme 9).[51]

Catalano and co-workers have also explored the luminescence properties of heteronuclear complexes synthesised from pyridine-substituted phosphine ligands.[55] Complex **29** was synthesised by reacting the P^{py} ligand L^{11} with Au(tht)Cl in 2 : 1 stoichiometric ratio followed by salt metathesis of the counter-ion using $NaBF_4$.[55] Reacting the gold(I) complex **29** with $[Cu(MeCN)_4](BF_4)$ in acetonitrile yielded complex **30**, which on further exposure to air resulted in the formation of complex **31**.[55] Complex **31** can also be crystallised by slow vapor diffusion of diethylether into a dichloromethane solution of complex **30**. Crystals of complex **30** were grown by slow diffusion of diethylether in acetonitrile solution. As expected, the gold(I) ion is coordinated to two phosphorous atoms and adapts a linear geometry in complex **30** and the copper(I) center features a distorted tetrahedral geometry by bonding to nitrogen atoms of two ligand units and two acetonitrile solvent molecules.[55] N–Cu–N bond angles vary between 97.68(6) to 138.68(6)°. Complex **31**, which is formed due to desolvation

Table 1 Excitation and emission maxima of complexes **15–23** in solid state.[20,22,45–47]

	λ_{ex} (nm)	λ_{em} (nm)
	298 K	298 K
15	340	416[a]
16	310	475 (br)[a]
17	398	512[a]
18	398	502[a]
19	398	507[a]
20	398	533[a]
21	365	462
22	365	461
23	346	455

[a] For complexes **15–20**, the values for the excitation maxima were extracted from the published graphs and thus are approximate values.

of complex **30**, varies from **30** in terms of geometry of the metal ions. Complex **31** features short Au–Cu distance of 2.886(2) Å when compared to complex **30** with Au–Cu distance of 3.3736(3) Å. Both gold(I) and copper(I) ions feature almost linear geometry wherein they are coordinated to two phosphorous and nitrogen atoms respectively. Complex **30** exhibits green luminescence which on desolvation demonstrates yellowish luminescence.[55]

The PN_4 ligand system ($\mathbf{L^{12}}$; Scheme 10), in which two bipyridine moieties are attached to a central phosphorus atom fulfils the prerequisites mentioned above,[48] just as the monoanionic PNNP ligand ($\mathbf{L^{13}}$; Scheme 11), introduced in 2002 by Tsukada *et al.*,[56] composed of a negatively charged amidinate as nitrogen center with two attached phosphine moieties.[57,58]

As expected, the reaction of $\mathbf{L^{12}}$ with a gold(I) precursor in a 2 : 1 ratio leads to the formation of a gold(I) complex linearly coordinated by two phosphorus atoms (**32**, Scheme 10). The stoichiometric addition of copper(I) (**33**) and silver(I) (**34**) precursors leads to trinuclear heterobimetallic complexes, filling the empty coordination compartment of the bipyridine moieties (Scheme 10).[48] Both complexes resemble each other, forming an almost linear arrangement of the three metal ions (*ca.* 179°), with tetrahedrally distorted coordinated silver(I) or copper(I) atoms. These two compounds show metallophilic interactions, having Au–M distances of around 3 Å for silver(I) as well as copper(I), implying that the range of the metal–metal distances are mainly a consequence of the rigid ligand geometry.[59–61]

A trinuclear homometallic silver(I) complex **35** was synthesized, displaying the identical structural arrangement as the two heterometallic compounds **33** and **34**. Here, silver(I) is coordinated by a significant more distorted tetrahedral geometry highlighted through the varying length of Ag–N bonds, which is greater than the corresponding gold(I)–silver(I) complex (Fig. 8).[48,62]

The reaction of coinage metal precursors with the potassium salt of the amidinate based PNNP ligand $\mathbf{L^{13}}$ (Scheme 11) leads to neutral dinuclear compounds, forming isostructural complexes with copper(I) (**36**) and silver(I) (**37**).[58] In contrast to $\mathbf{L^1}$–$\mathbf{L^{12}}$, ligand $\mathbf{L^{13}}$ is an anionic ligand, which leads to metal complexes with an overall lower charge. In general, these are

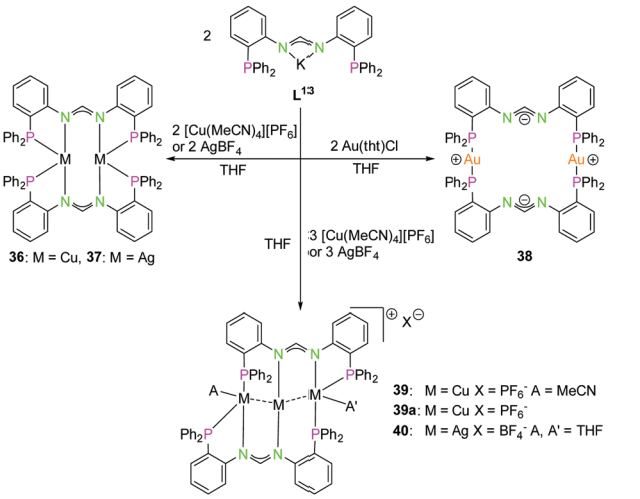

Scheme 11 Synthesis of di- (**36–38**) and trinuclear (**39**, **39a**, **40**) homometallic PNNP (K–$\mathbf{L^{13}}$) compounds.[58]

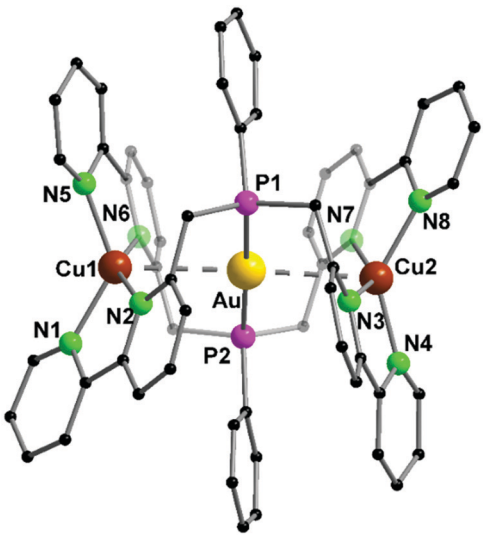

Fig. 8 Molecular structure of **33** in the solid state. Hydrogen atoms and the counter ions are omitted for clarity.[48]

better soluble in organic solvents than their highly charged counterparts **32–34**. The metal atoms in **36** and **37** are each coordinated by two nitrogen atoms and two phosphorous atoms in a distorted tetrahedral environment. Although bis(amidinate) copper(I) complexes similar to **36** are known to form short Cu–Cu contacts, no cuprophilic interaction is observed (3.63 Å) in **36**,[63,64] most likely since the phosphine moiety allows the more favoured tetrahedral coordination. In contrast an intermetallic distance of 3.44 Å indicates weak argentophilic interactions for the dinuclear silver(I) complex **37** in good agreement with literature values.[9]

Despite literature known dinuclear gold(I) bis(amidinate) compounds with gold(I) coordinated by two nitrogen atoms,[65,66] the structure of **38** is differing significantly from these and from structures with the lower homologues.

A slightly bent bis(phosphine) gold(I) coordination mode is obtained, showing the preference of gold(I) for soft donors and low coordination numbers. A remarkable charge separation was observed for compound **38**, with the negative charges delocalised over the NCN and the positive charges situated on the gold(I) atoms.[58,67] With a ligand to reactant ratio of 2 : 3 it is possible to synthesise trinuclear homometallic complexes (**39**, **40**), revealing a tilted Cu_3 chain (117.84(1)°) (Scheme 11). All three copper(I) atoms are in different coordination modes, not taking the cuprophilic interactions into account. Cu1 is almost trigonal planar coordinated, Cu2 is almost linearly coordinated and Cu3 is additionally coordinated by one molecule of acetonitrile, resulting in a distorted tetragonal coordination.

Due to the different coordination geometries of the metal ions intermetallic distances are varying, leading to a short 2.5984(4) Å (Cu1–Cu2) and a longer 2.7792(4) Å (Cu2–Cu3) interaction.[8,58] Crystallisation in absence of MeCN leads to a similar scaffold with a bent Cu_3 chain (**39a**) (122.07(3)°) and both outer copper(I) atoms are distorted trigonal planar coordinated. This results in a roughly similar Cu–Cu distance (*ca.* 2.56 Å) between the outer and the central copper(I) atoms. Finally, the homologue silver(I) complex was synthesised (**40**), showing a weakly bound THF at both outer silver(I) atoms, giving a more symmetrical arrangement than for the copper(I) (MeCN) compound **39**, with the Ag_3 chain slightly more bent (133.861(10)°) and intermetallic distances around 2.89 Å.[9,58]

The dinuclear gold(I) compound **38**, mentioned above (Scheme 11), still has open coordination sites and addition of coinage metal precursors resulted in three tetranuclear coinage metal chain complexes (**41**–**43**) (Scheme 12).[57] The inner lying atoms of the heterometallic complexes (**41**, **42**) are each coordinated by two nitrogen atoms and one THF molecule forming a trigonal planar coordination or, if the intermetallic interactions are taken into account, a distorted trigonal bipyramidal coordination. The gold(I) atoms in all three compounds are almost linear coordinated by two phosphorous atoms and almost planar T-shaped considering the Au–M contact, respectively. In contrast to the heterometallic compounds, the inner gold(I) atoms of the tetranuclear homometallic compound **43** are not coordinated by solvent molecules consequently having an almost linear coordination. The average intermetallic angle M–M–M is almost identical for the copper(I) and silver(I) compound (121.92° Cu; 119.42° Ag) but significantly widened for gold(I) (131.63°).[57]

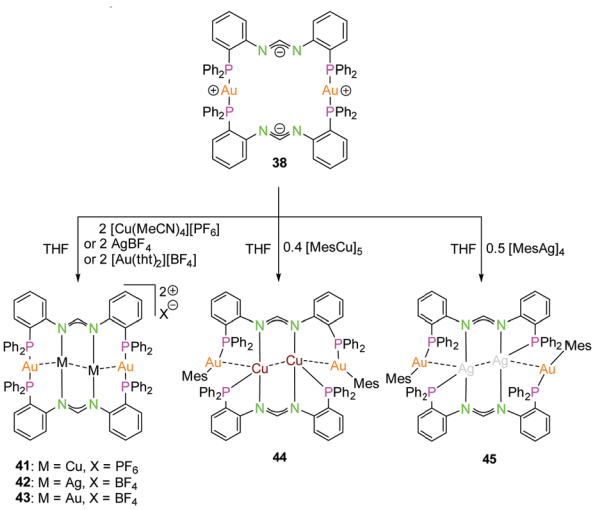

Scheme 12 Synthesis of tetranuclear hetero- (**41**, **42**, **44**, **45**) and homometallic (**43**) PNNP (**L**[13]) compounds.[57,68]

It should be mentioned, that even through gold(I) prefers soft donor sites, a coordination by hard nitrogen donors is possible with enough stabilisation.[66,69] A trend can be observed for the intermetallic distances. The outer Au–M contacts are in a range of 2.8 Å to 2.9 Å with the order Ag(I) > Au(I) > Cu(I), also similar for the inner metallophilic interaction (2.7334(2) Å Ag; 2.6998(8) Å Au; 2.5995(3) Å Cu). This shows, that even though gold(I) has the greater van der Waals radii than silver(I), it forms stronger interactions with smaller intermetallic distances.[57,70–73] The metalloligand **38**, when reacted with mesityl copper(I) and mesityl silver(I) in THF, resulted in the tetranuclear heterometallic complexes **44** and **45** in 36% and 33% yield respectively (Scheme 12).[68] Both complexes were crystallised from THF and *n*-pentane. Molecular structure of **44** in the solid state revealed that each inner lying copper(I) atom is coordinated to two nitrogen atoms of the amidinate group and to a phosphine unit in an almost T-shaped geometry.[68] The metals arrange themselves in a Au–Cu–Cu–Au zigzag chain with an angle of 111.62(2)° and intermetallic distances of 2.7939(9) Å (Cu–Cu) and 2.9960(4) Å (Au–Cu) which are in the range of metallophilic interactions. Following the HSAB principle, gold coordinates to phosphorous and a mesityl unit. Additionally, gold deviates from its usual linear geometry with an angle of 167.67(10)° (P–Au–mesityl).[68] Complex **45** also demonstrates a rather similar tetranuclear zigzag chain Au–Ag–Ag–Au wherein the intermetallic bond distances are 2.9756(3) Å (Au–Ag) and 2.9009(5) Å (Ag–Ag) and the bond angle is 102.197(13)°.[68]

In contrast to Au–Cu complex **44**, the mesityl groups which are exchanged from silver(I) to gold(I) atoms are located on the opposing ligand (Scheme 12). Each gold(I) atom in complex **45** is coordinated to a phosphorous and a mesityl unit, thereby adapting an almost linear geometry (173.80(10)°). Similar to complex **44**, the inner lying silver(I) atoms are coordinated by two nitrogen atoms and a phosphorous moiety and when metallophilic interactions are taken into consideration, silver(I) atoms are in an overall trigonal bipyramidal coordination environment. However, due to low solubility of the complexes, NMR investigations are not reported (Fig. 9).[68]

Scheme 13 displays several P–N ligands **L**[14]–**L**[18] containing a diphenyl phosphine unit as a soft donor and a phenanthrene (**L**[14]), aniline (**L**[15]), napthtyridine (**L**[16]), imidazole (**L**[17]), or a triazole (**L**[18]) function as hard nitrogen donor. Their complexes **46**–**51** can be synthesised straight forward by addition of the corresponding coinage metal precursors in a stoichiometric manner.[34,50,54,74,75] Complex **46** consists of two gold(I) ions, coordinated by the diphenyl phosphine and a $C_6Cl_2F_3$ in an almost linear fashion, and a copper(I) core coordinated by the

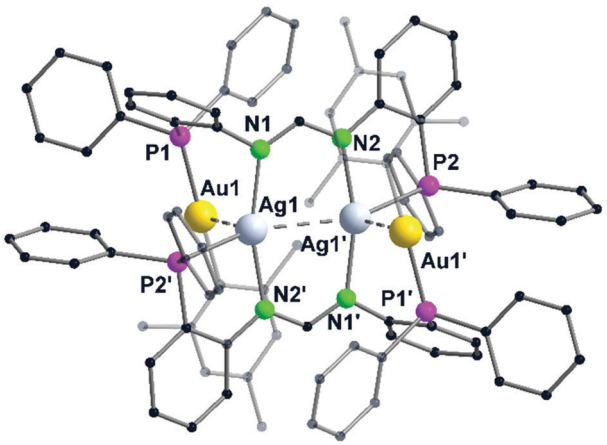

Fig. 9 Molecular structure of **45** in the solid state. Hydrogen atoms and the counter ions are omitted for clarity.[68]

two nitrogen atoms of phenantrene and an acetonitrile molecule in a distorted trigonal conformation. The rigid ligand geometry prevents the close association of the metal centers, thus no metal interactions in the solid state can be noted.[54] The dinuclear compounds **47** and **48** are closely related. Herein, the gold(I) is coordinated by the two phosphorus atoms in a linear manner, and the second metal ion by two nitrogen donors. The Au–Ag distance is *ca.* 3.0 Å.[74] Compound **49** shows a trigonal coordination of both metal ions gold(I) and copper(I) forming almost parallel plains (P_3Au, N_3Cu). Copper is coordinated by the second nitrogen of the napthtyridine, thus resulting in a long Au–Cu distance of 4.47 Å.[34] Similar to compound **49**, complex **50** has trigonal coordinated metal ions. The highly symmetrical compound **50** has intermetallic interactions with a distance of 2.86 Å (Au–Ag). Experiments to synthesise the linear coordinated species with ligand **L**[17] were unsuccessful and only works for the homometallic gold(I) and silver(I) compounds.[50] At last, compound **51** having a similar solid state structure as **24** and **26**, but with a slightly elongated Au_2Cu core (Au–Au 3.48 Å, Au–Cu 3.06–3.20 Å) and copper(I) is additionally coordinated by two thf molecules.[13,75] Interestingly the ligand L[18] can not only be used as a P–N orthogonal ligand but also as P–C ligand by alkylating the nitrogen donor and deprotonation to the mesoionic carbene species or by deprotonation to the triazolide. The resulting soft–soft coordination sites are capable of building dinuclear homometallic gold(I) compounds.[75]

The structures depicted in Scheme 13 show compounds with trigonal planar coordinated (**46**, **49**, **50**) as well as linear coordinated (**46–48**) coinage metals. In particular, compounds **47**, **48** and **50** show that linear or trigonal coordination can be modulated by the ligand system, respectively.

Depicted in Scheme 14 is the synthesis of the tetranuclear bimetallic gold(I)–copper(I) compound **53** using the $(PPh_2)_2Py$ ligand **L**[19]. Simple addition of 2 equiv. of $Cu(SMe_2)Br$, followed by silver(I)triflate leads to the dinuclear copper() compound **52**, which can be converted to **53** by transmetalation with $Au(SMe_2)Cl$. Compound **53** has linear coordinated gold(I) ions bridging the two ligand moieties, copper(I) rises above and below the paper plane and is linear coordinated by the pyridine nitrogen and one chloride. The gold(I)–copper(I) intermetallic distance is between 3.034 and 3.065 Å and the Au_2Cu_2 core forms a tetranuclear planar shaped metal alternating tetragon.[18]

Like above-mentioned for C–N coordination, the combination of soft phosphorous and hard nitrogen donor sites also allows a selective coordination of coinage metals. The advantage of these selectivity is reflected by the changes in the PL properties with different metal loadings and coordination spheres.

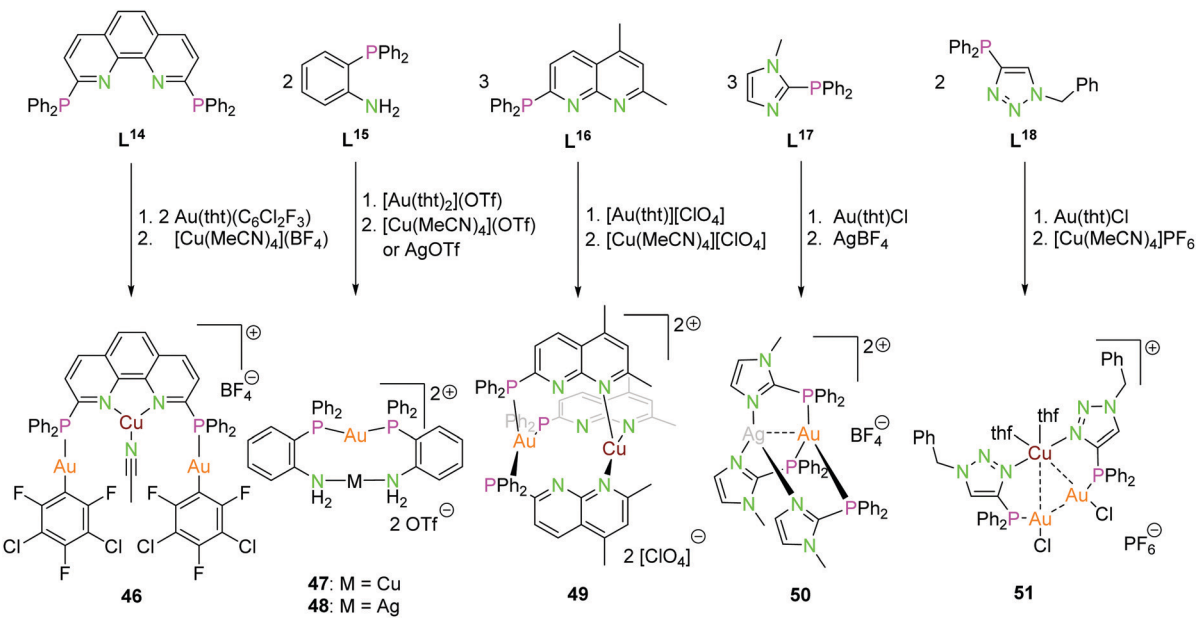

Scheme 13 Synthesis of heterometallic di- (**47–50**) and trinuclear (**46**, **51**) compounds with ligands **L**[14]–**L**[18].[34,50,54,74,75]

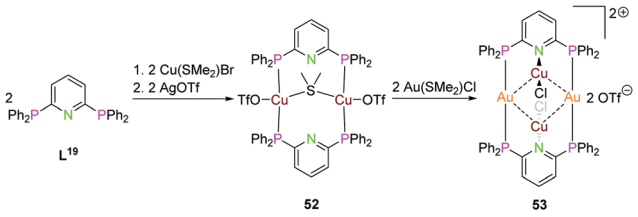

Scheme 14 Synthesis of homo- (**52**) and heterometallic (**53**) compounds with ligand $\mathbf{L^{20}}$.[18]

Photoluminescence properties

Metalloligands $\mathbf{L^7}$–$\mathbf{L^{10}}$ do not exhibit luminescence at ambient temperature. However, on introducing copper(I) as a hetero metal, the complexes exhibit different emissive behaviour.

Complexes **24–27** (Table 2) in the solid-state exhibit broad emission band centered at 516 nm, 542 nm, 450 nm (broad shoulder at approx. 550 nm) and 558 nm at room temperature respectively.[47,51] The lifetimes for these complexes **24** and **27** at room temperature are measured to be 29 μs and 13 μs respectively indicating phosphorescent nature.[13] The emission of complex **26** at 297 K is also phosphorescent in nature, resulting from minimum of two non-equilibrated triplet states with lifetimes of τ_{450nm} = 2.2(77)/6.3(23) μs and τ_{550nm} = 12 μs (pre-exponential factors are mentioned in brackets). In contrast to complexes **24–27**, the emission band of **28** appears at lower energy, which is attributed to the different coordination geometry of copper(I) (tetrahedral).[13] Heterometallic complex **30** shows blueish emission in acetonitrile solution (λ_{max} = 367, 389 nm (shoulder)) and intense emerald colour (λ_{max} = 412 nm) in the solid state.[55] Complex **31** which formed due to loss of acetonitrile solvent molecules from **30** features thermochromism behaviour (*i.e.*, exhibits different emission colours at different temperatures) in the solid-state. It emits intense, yellow-coloured emission at 298 K, with the emission band centred at λ_{max} = 551 nm and when heated to 343 K, λ_{max} is shifted to 536 nm (aquamarine), due to endothermic phase transition and remains unchanged above 343 K. On cooling the sample to 77 K the emission is green coloured with λ_{max} = 543 nm, which is attributed to rigidochromism (mechanical sensitivity). The thermochromism behaviour is reversible and is maintained for more than five heating/cooling cycles (Table 2).[55] The PN_4 compounds **32–35** (Scheme 10) show roughly similar broad emission with a slightly visible vibronical structure for the mononuclear gold(I) complex **32** with the highest intensity at 520 nm (Fig. 10). The heterometallic trinuclear gold(I)–silver(I) complex **34** has a bathochromic shift to 580 nm and the gold(I)–copper(I) compound **33** is shifted further to 740 nm in the NIR region due to the HOMO contribution from the d-orbitals of copper(I). Also, the PL onset at about 720 nm leads to the deep-red colour, while the other trinuclear compounds **34** and **35** have a PLE onset at 400–450 nm. The replacement of gold(I) with silver(I) in the homometallic trinuclear silver(I) complex **35** shows no impact on the PL properties (Fig. 10).[48] PL spectra of dinuclear compounds **36–38** (Scheme 11) look quite identical, with similar PLE spectra onset at *ca.* 450 nm (Fig. 6). The vibronically structured emission is similar for copper(I) (**36**) and silver(I) (**37**), with emissions around 520 nm, but since the gold(I) compound **38** has a structural difference, the PL spectra shows a distinct spectrum with a blueshift of the emission (Fig. 11).[58] Both trinuclear complexes of copper(I) **39** and **39a** (Scheme 11) show similar PLE spectra with onset at 450 nm and PL emission at *ca.* 500 nm, but the shape of the PL spectra is different (Fig. 6). The Cu(MeCN) complex **39** shows a vibronic pattern, while it is absent without coordinating solvent (**39a**), leading to the conclusion that the vibronic "modulation" can be attributed to the acetonitrile coordination. Accordingly, the silver(I) compound **40** (Scheme 11) with coordinating THF molecules shows no vibronic pattern but is significantly blueshifted towards 460 nm with a PLE onset at 360 nm (Fig. 11).[57,58] Fig. 12 shows the PL spectra of the tetranuclear complexes **41–43** (Scheme 12), all having broad (especially the copper(I) compound **41**) emission maxima, with a significant bathochromic shift from silver(I) (**42**) (430 nm) to gold(I) (**43**) (490 nm) to copper(I) (**41**) (530 nm). This bathochromic shift of copper(I) and blueshift of silver(I) relatively to gold(I) is in overall accordance with the behaviour of the other described compounds when the coinage metal composition is changed.[57]

Complexes **44** and **45** exhibit broad emission bands both at ambient and low temperatures in the solid-state with a

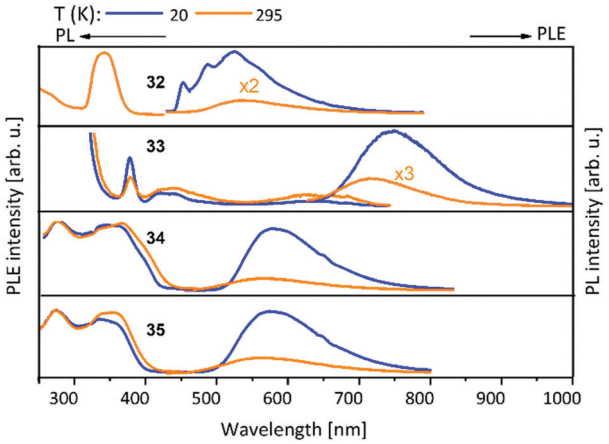

Fig. 10 Solid state excitation and emission spectra of PN_4 ($\mathbf{L^{12}}$) metal complexes **32–35**. PL was excited at λ_{exc} = 350 nm and PLE spectra recorded at λ_{em} = 560 nm for **32**, **33**, **35** and λ_{em} = 580 nm for **34**.[48]

Table 2 Solid state photophysical properties of complexes **24–28**, **30** and **31**.[13,51,54,55]

	λ_{ex} (nm)	λ_{em} (nm)	τ_{obs} (μs)	Φ_{em} (%)
	298 K	298 K	298 K	298 K
24	320, 360	558 (+sh)	29	—
25	390	542	2.82	14
26	350	450, 550 (sh)	2.2(7.7)/6.3(23) 12	28.0
27	360	516 (br)	13	—
28	460	715	—	—
30	350	536	—	—
31	350	551	—	—

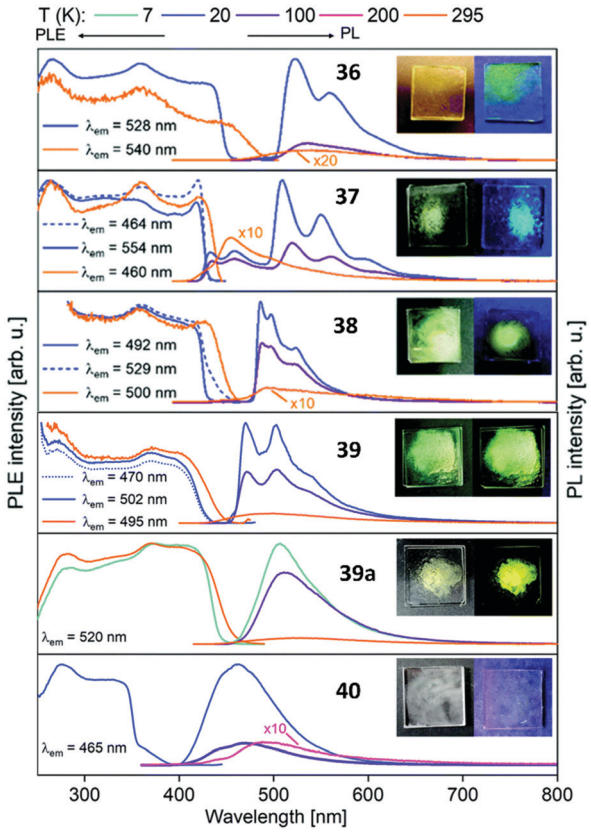

Fig. 11 Solid state excitation and emission spectra of di- and trinuclear PNNP (L^{13}) metal complexes **36–40**. PL was excited at λ_{exc} = 350 nm for **36–39a** and λ_{exc} = 330 nm for **40**.[58]

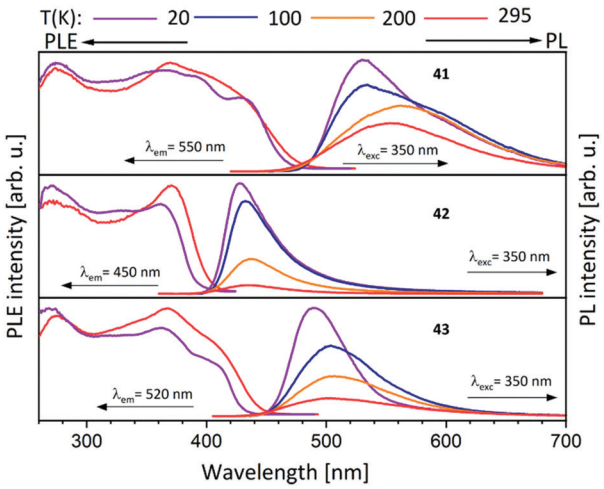

Fig. 12 Solid state excitation and emission spectra of tetranuclear PNNP (L^{13}) metal complexes **41–43**.[57]

maximum at 600 nm and 482 nm respectively (Table 3).[68] Like previously discussed complex **33**,[48] a bathochromic shift in the PL spectra is observed for the copper(I) complex **44**.[68] The quantum yields of compounds **44** and **45** were reported to be 35% and 2% respectively and the PL efficiency reaches nearly

Table 3 Solid state photophysical properties of complexes **44–46**, **50**, **51** and **53**[50,54,68,75]

	λ_{ex} (nm) 298 K	λ_{em} (nm) 298 K	τ_{obs} (μs) 298 K	77 K	Φ_{em} (%) 298 K
44	350	600	—	310	35
45	350	482	—	320	5
46	455	615	2.7/0.7	—	8
50	360	490	—	—	—
51	350	580	8	14	9
53	334	490	7.7		12

100% at temperatures below 100 K (Table 3).[68] Complexes **44** and **45** are phosphorescent, and the lifetimes are measured to be 310 μs for **44** and ca 320 μs for **45** at 20 K. However, the lifetimes tend to decrease with an increase in temperature.[68] Additionally, we want to mention the observation of a bathochromic shift for compounds **41** and **43** when measured in the gas phase, solution and solid state. TDDFT calculations showed, that the electronic properties of Au–M–M–Au complexes can be strongly modulated by metallophilic Au–M interactions. The remarkable agreement of experimental and calculated energies of ionic compounds in gas phase demonstrate the importance of gas phase PL spectroscopy combined with quantum chemical calculations.[57]

Phenantrene compound **46** shows a broad asymmetric band at 615 nm, with biexponential decay times τ = 2.7/0.7 μs and a quantum yield φ(295 K) of 8% in the solid state (Table 3). In THF solution a structured emission at 436 nm can be observed (Table 4), possibly due to the coordination of solvent, like for compound **39**.[54,58] Compounds **47** and **48** both have featureless bands at 431 nm (Au–Cu) and 430 nm (Au–Ag) (Table 4).[74] The trigonal gold(I)–copper(I) compound **49** exhibits an emission band at 530 nm and is blueshifted in comparison to the mononuclear gold compound (560 nm) (Table 4).[34] The second trigonal compound **50** shows a broad featureless band at 490 nm in the solid state and a blueshifted single emission band at 354 nm.[50] Compound **51** displays a broad featureless emission band centered at 580 nm, typical for charge transfer transitions. The emission decay are τ = 14 μs and 8 μs at 20 K and 295 K, respectively and the quantum yield φ(295 K) is 9% (Table 3).[75] Compound **53** shows abroad peak at 490 nm with a lifetime of 7.7 μs and a quantum yield φ(295 K) of 11.8% (Table 3).[18]

P–O coordination

Coordination modes

Following Pearsons' concept of HSAB principle, combination of P- and O-donor sites presents an additional class of bifunctional ligands which fulfils the pre-requisite for the synthesis of heterobimetallic complexes, with oxygen being a hard donor, preferring coordination with copper(I) as well as silver(I). Koshevoy and co-workers have reported a series of coinage metal complexes using a mixed phosphine–phosphine oxide (P–PO) hybride ligand.[76] However, to the best of our knowledge, there has been no other coinage metal complexes reported with

Table 4 Excitation andemission maxima of heteronuclear complexes **46–50** in solution.[34,74]

	λ_{ex} (nm)	λ_{em} (nm)
	298 K	298 K
46	373	436
47	350	600
48	350	482
49	455	615

P–O bifunctional ligands, which are studied with respect to their optical properties. The limited study corresponding to this class of ligands is attributed to the challenging synthesis and low selectivity of unsymmetrical oxide derivates when compared to their parent phosphines (Scheme 15).[76]

Koshevoy and co-workers were successful to synthesize bis(triphenylphosphine)phenylphosphanoxide ($\mathbf{L^{20}}$) in 80% yield. Ligand $\mathbf{L^{20}}$ was employed for the synthesis of several homometallic complexes and a heterobimetallic complex (Scheme 14).[76]

The heterobimetallic complex **57** was synthesized by reacting the homometallic complexes **54** and **56** in DCM for 2 h. The complex was isolated as yellow crystalline solid in 84% yield. The molecular structure in the solid state was established using single crystal XRD analysis. $\mathbf{L^{20}}$ being a tridentate ligand, provides two types of ligand spheres in the complex **57** ("P_2O_2" and "P_2"). The ligand sphere P_2O_2 includes a phosphine group and phosphine oxide of two ligand moieties, which accommodates Cu(I) ion and the P_2 ligand sphere is comprised of the other phosphine functionality of the ligand, which saturates the coordination vacancy of Au(I). Copper(I) is coordinated by the lone pairs of phosphorous and oxygen atoms, adopting a distorted tetrahedral coordination geometry. Whereas gold(I), coordinated by two phosphorous atoms, slightly deviates from ideal linear geometry, which is attributed to weak Au–O interactions. Silver(I), with its behaviour in between, coordinates only to one oxygen atom and is additionally weakly η^2 coordinated to a C=C double bond of a phenyl ring, leading to a strongly distorted tetrahedral coordination.[76] The purity of the complexes was established using NMR spectroscopic measurements and elemental analysis. NMR investigation of compound **57** revealed the presence of a dynamic equilibrium in solution between heterobimetallic complex **57**

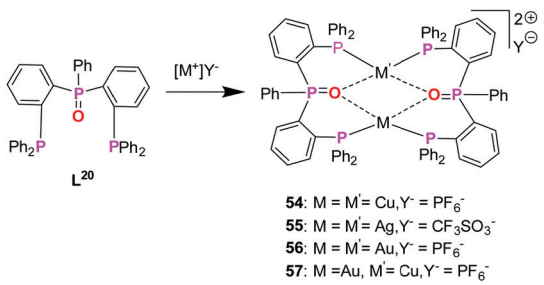

Scheme 15 Synthesis of homo- (**54–56**) and heterometallic (**57**) complexes based on mixed phosphine–phosphine oxide hybrid ligand ($\mathbf{L^{20}}$).[76]

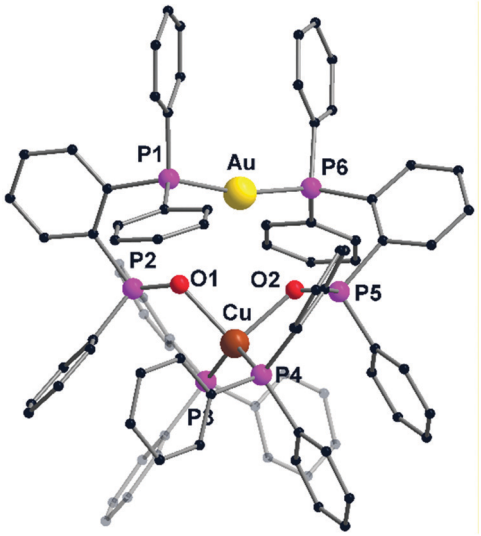

Fig. 13 Molecular structure of **57** in the solid state. Hydrogen atoms and the counter ions are omitted for clarity.[76]

and its homometallic congeners. However, on recrystallisation of the mixture, crystals of complex **57** can be recovered which was characterized by XRD analysis. Additionally, complex **57** shows a unique emission spectrum which is different from its homometallic congeners which supports the analytical purity of **57** (Fig. 13).[76]

Photoluminescence properties

The complexes **54–57** (Scheme 14) do not exhibit significant luminescence in solution, hence, only the solid state photophysical properties are summarised in Table 5. Well-reported bathochromic shift for copper(I) complex **54** and hypsochromic shift of silver(I) complex **55** relative to gold(I) complex **56** is observed. Gold(I)–copper(I) complex **57** displays a broad emission band centered at 538 nm. The emission band of **57** is blue shifted with respect to the emission spectra of **54** and **56** which are centred at 604 and 548 nm, respectively. Gold(I) containing complexes **56** and **57** exhibit comparatively larger quantum efficiencies due to increased radiative rate constants. The effect is mainly due to larger spin orbit coupling present in gold(I) complexes and a higher inter system crossing (ISC) rate when compared to their first and second row transition metal complexes.[76] The lifetime for complexes **54–57** is in the microseconds range at 298 K which drastically increases on lowering the temperature to 77 K. Heterobimetallic complex **57** doesn't

Table 5 Solid state photophysical properties of P^3O ($\mathbf{L^{20}}$) complexes **54–57**.[76]

	λ_{ex} (nm)	λ_{em} (nm)	τ_{obs} (μs)		Φ_{em} (%)
	298 K	298 K	298 K	77 K	298 K
54	364	604	0.35	174.1	0.5
55	332	500	10.9	2354.3	5.9
56	330	548	6.7	82.3	28.9
57	360	538	5.5	777.5	25.8

exhibit any significant difference in terms of quantum yield and lifetime when compared with **54** and **56** at 298 K. However, the lifetime for complex **57** at 77 K is 777.5 μs which is considerably greater than the homometallic analogues **54** (174.1 μs) and **56** (82.3 μs).[76]

Conclusions

The selective coordination of transition metals can be achieved by using hard and soft donor sites following the HSAB principle of Pearson. For the selective coordination of several different metals to the same ligand system, specially designed ligand systems are needed. The combination of C–N, P–N or P–O coordination sites in the same ligand, resulting in orthogonal ligands, is one way to achieve this. The specific preferences of the coinage metals allow the synthesis of multinuclear heterometallic complexes, where the metal can be selectively coordinated to different donor sites.

Copper(I) prefers hard donor sites, with high coordination numbers, and can be found in tetrahedral, trigonal planar but also in linear coordination modes. The same applies to silver(I) but a propensity to lower coordination numbers and the formation of intermetallic interactions can be noted. Finally, gold(I) as soft metal coordinates to soft donor functions with low coordination numbers. It can be said that all featured ligand systems C–N, P–N and P–O show the expected selectivity and therefore are good examples for orthogonal ligand designs. Besides the fixation of orthogonal donor sites, the ligand architecture is also essential for the nuclearity of the corresponding complexes. We have shown examples ranging from bi- to tetranuclear complexes.

Another outstanding property of the coinage metals is their propensity to form strong intermetallic interactions, known as metallophilicity. This increases the interest in the formation of heterometallic multinuclear coinage metal complexes. With the metals in close range to each other, the influence of the variable metal loading on their coordination behaviour as well as the intermetallic exchange can be investigated.

It must be mentioned that the metallophilic interactions also have an impact on the PL properties and can be easily tuned by exchange of the metal loading. Thus, copper(I) containing compounds usually experience a bathochromic shift while silver(I) tends to a hypsochromic shift.

Overall, there are many ligand systems with C–N and P–N donor sites, but not many findings for P–O orthogonal ligands. Additionally, sulphur, in combination with nitrogen or oxygen presents an excellent class of orthogonal ligands. There are only a few examples of such ligands. Konno *et al.* synthesised multimetallic homo- and heteronuclear metallorings from benzothiazoline.[77] However, the optical properties of the metal complexes were not reported. Other sulphur containing ligands are of C–S type, with the combination of thiophene and NHC's, giving good soft coordination sites and are explored by Cavell and co-workers.[78,79] Both of the works present good examples for the potential of sulphur in the coordination chemistry of coinage metal and provide a scope to develop other sulphur based orthogonal ligands, which can be further studied in terms of their coordination behaviour and photoluminescence properties. These examples show that many combinations in terms of hard soft interaction exists, which are not explored yet.

In the future, we expect a better understanding of the structure property relationship of these kind of compounds due to the increasing power of theoretical methods. This facilitates the task specific assembly of compounds showing a desired emission. Thus, on the long run, we expect that the emission colour can be adjusted by a rational synthesis, which is directed by theoretical predications.

Author contributions

VRN and FR did the literature research and wrote most parts of the manuscript. PWR originated the idea and supervised the work. All authors contributed to the preparation of the manuscript.

Conflicts of interest

The authors declare no conflict of interest.

Acknowledgements

We want to thank Niklas Reinfandt for proofreading the manuscript. The Deutsche Forschungsgemeinschaft (DFG) funded Research Training Group (RTG) 2039 (Molecular architecture for fluorescent cell imaging) is acknowledged for financial support of VRN. The DFG funded Transregional Collaborative Research Centre 88 [Cooperative Effects in Homo- and Heterometallic Complexes (3MET)], Projects C3, is acknowledged for financial support of FK.

Notes and references

1 V. W.-W. Yam, V. K.-M. Au and S. Y.-L. Leung, *Chem. Rev.*, 2015, **115**, 7589–7728.
2 S. Raju, H. B. Singh and R. J. Butcher, *Dalton Trans.*, 2020, **49**, 9099–9117.
3 H. Schmidbaur and A. Schier, *Chem. Soc. Rev.*, 2012, **41**, 370–412.
4 F. Scherbaum, A. Grohmann, G. Müller and H. Schmidbaur, *Angew. Chem., Int. Ed. Engl.*, 1989, **28**, 463–465.
5 H. Schmidbaur, *Gold Bull.*, 1990, **23**, 11–21.
6 M. Jansen, *Angew. Chem., Int. Ed. Engl.*, 1987, **26**, 1098–1110.
7 N. V. S. Harisomayajula, S. Makovetskyi and Y. C. Tsai, *Chem. – Eur. J.*, 2019, **25**, 8936–8954.
8 H. L. Hermann, G. Boche and P. Schwerdtfeger, *Chem. – Eur. J.*, 2001, **7**, 5333–5342.
9 H. Schmidbaur and A. Schier, *Angew. Chem., Int. Ed.*, 2015, **54**, 746–784.
10 M. Jansen, *J. Less-Common Met.*, 1980, **76**, 285–292.
11 J. M. López-de-Luzuriaga, M. Monge, M. E. Olmos, D. Pascual and M. Rodríguez-Castillo, *Organometallics*, 2012, **31**, 3720–3729.
12 J. M. López-De-Luzuriaga, M. Monge, M. E. Olmos, J. Quintana and M. Rodríguez-Castillo, *Inorg. Chem.*, 2019, **58**, 1501–1512.
13 M. J. Calhorda, C. Ceamanos, O. Crespo, M. C. Gimeno, A. Laguna, C. Larraz, P. D. Vaz and M. D. Villacampa, *Inorg. Chem.*, 2010, **49**, 8255–8269.

14 A. Laguna, T. Lasanta, J. M. López-De-Luzuriaga, M. Monge, P. Naumov and M. E. Olmos, *J. Am. Chem. Soc.*, 2010, **132**, 456–457.
15 Q. Wan, J. Yang, W.-P. To and C.-M. Che, *Proc. Natl. Acad. Sci. U. S. A.*, 2021, **118**, e2019265118.
16 M. B. Brands, J. Nitsch and C. F. Guerra, *Inorg. Chem.*, 2018, **57**, 2603–2608.
17 S. Sculfort and P. Braunstein, *Chem. Soc. Rev.*, 2011, **40**, 2741–2760.
18 S. Nayeri, S. Jamali, A. Jamjah and H. Samouei, *Inorg. Chem.*, 2019, **58**, 12122–12131.
19 Z. Lei, S.-S. Chang and Q.-M. Wang, *Eur. J. Inorg. Chem.*, 2017, 5098–5102.
20 C. E. Strasser and V. J. Catalano, *J. Am. Chem. Soc.*, 2010, **132**, 10009–10011.
21 K. N. Jarzembska, R. Kamiński, K. F. Dziubek, M. Citroni, D. Paliwoda, K. Durka, S. Fanetti and R. Bini, *Inorg. Chem.*, 2018, **57**, 8509–8520.
22 K. Chen, M. M. Nenzel, T. M. Brown and V. J. Catalano, *Inorg. Chem.*, 2015, **54**, 6900–6909.
23 N. Glebko, T. M. Dau, A. S. Melnikov, E. V. Grachova, I. V. Solovyev, A. Belyaev, A. J. Karttunen and I. O. Koshevoy, *Chem. – Eur. J.*, 2018, **24**, 3021–3029.
24 X. L. Pei, Z. J. Guan, Z. A. Nan and Q. M. Wang, *Angew. Chem.*, 2021, **133**, 14502–14505.
25 V. W.-W. Yam and K. K.-W. Lo, *Chem. Soc. Rev.*, 1999, **28**, 323–334.
26 R. Jazzar, M. Soleilhavoup and G. Bertrand, *Chem. Rev.*, 2020, **120**, 4141–4168.
27 J. C. Y. Lin, R. T. W. Huang, C. S. Lee, A. Bhattacharyya, W. S. Hwang and I. J. B. Lin, *Chem. Rev.*, 2009, **109**, 3561–3598.
28 A. V. Paderina, I. O. Koshevoy and E. V. Grachova, *Dalton Trans.*, 2021, **50**, 6003–6033.
29 V. W.-W. Yam and K. M.-C. Wong, *Chem. Commun.*, 2011, **47**, 11579.
30 C. Fliedel, A. Ghisolfi and P. Braunstein, *Chem. Rev.*, 2016, **116**, 9237–9304.
31 A. Belyaev, T. M. Dau, J. Jänis, E. V. Grachova, S. P. Tunik and I. O. Koshevoy, *Organometallics*, 2016, **35**, 3763–3774.
32 R. G. Pearson, *J. Chem. Educ.*, 1968, **45**, 643.
33 R. G. Pearson, *Inorg. Chim. Acta*, 1995, **240**, 93–98.
34 W. H. Chan, K. K. Cheung, T. C. W. Mak and C. M. Che, *J. Chem. Soc., Dalton Trans.*, 1998, 873–874.
35 Y.-Y. Lin, S.-W. Lai, C.-M. Che, Fu, Z.-Y. Zhou and N. Zhu, *Inorg. Chem.*, 2005, **44**, 1511–1524.
36 A. Belyaev, T. Eskelinen, T. M. Dau, Y. Y. Ershova, S. P. Tunik, A. S. Melnikov, P. Hirva and I. O. Koshevoy, *Chem. – Eur. J.*, 2018, **24**, 1404–1415.
37 Z. Lei, X.-L. Pei, Z.-J. Guan and Q.-M. Wang, *Angew. Chem., Int. Ed.*, 2017, **56**, 7117–7120.
38 L.-Q. Mo, J.-H. Jia, L.-J. Sun and Q.-M. Wang, *Chem. Commun.*, 2012, **48**, 8691.
39 X.-Y. Liu, Y. Yang, Z. Lei, Z.-J. Guan and Q.-M. Wang, *Chem. Commun.*, 2016, **52**, 8022–8025.
40 S. Nayeri, S. Jamali, A. Jamjah, J. R. Shakirova, S. P. Tunik, V. Gurzhiy, H. Samouei and H. R. Shahsavari, *Inorg. Chem.*, 2020, **59**, 5702–5712.
41 C. Kaub, S. Lebedkin, A. Li, S. V. Kruppa, P. H. Strebert, M. M. Kappes, C. Riehn and P. W. Roesky, *Chem. – Eur. J.*, 2018, **24**, 6094–6104.
42 C. Kaub, S. Lebedkin, S. Bestgen, R. Köppe, M. M. Kappes and P. W. Roesky, *Chem. Commun.*, 2017, **53**, 9578–9581.
43 T. Simler, K. Möbius, K. Müller, T. J. Feuerstein, M. T. Gamer, S. Lebedkin, M. M. Kappes and P. W. Roesky, *Organometallics*, 2019, **38**, 3649–3661.
44 E. Fogler, E. Balaraman, Y. Ben-David, G. Leitus, L. J. W. Shimon and D. Milstein, *Organometallics*, 2011, **30**, 3826–3833.
45 V. J. Catalano, M. A. Malwitz and A. O. Etogo, *Inorg. Chem.*, 2004, **43**, 5714–5724.
46 C. E. Strasser and V. J. Catalano, *Inorg. Chem.*, 2011, **50**, 11228–11234.
47 V. J. Catalano and A. L. Moore, *Inorg. Chem.*, 2005, **44**, 6558–6566.
48 S. Schäfer, M. T. Gamer, S. Lebedkin, F. Weigend, M. M. Kappes and P. W. Roesky, *Chem. – Eur. J.*, 2017, **23**, 12198–12209.
49 S. Bestgen, M. T. Gamer, S. Lebedkin, M. M. Kappes and P. W. Roesky, *Chem. – Eur. J.*, 2015, **21**, 601–614.
50 V. J. Catalano and S. J. Horner, *Inorg. Chem.*, 2003, **42**, 8430–8438.
51 E. Hobbollahi, M. List, B. Hupp, F. Mohr, R. J. F. Berger, A. Steffen and U. Monkowius, *Dalton Trans.*, 2017, **46**, 3438–3442.
52 K. N. Jarzembska, R. Kamiński, B. Fournier, E. Trzop, J. D. Sokolow, R. Henning, Y. Chen and P. Coppens, *Inorg. Chem.*, 2014, **53**, 10594–10601.
53 I. O. Koshevoy, J. R. Shakirova, A. S. Melnikov, M. Haukka, S. P. Tunik and T. A. Pakkanen, *Dalton Trans.*, 2011, **40**, 7927.
54 V. J. Catalano, J. M. López-De-Luzuriaga, M. Monge, M. E. Olmos and D. Pascual, *Dalton Trans.*, 2014, **43**, 16486–16497.
55 K. Chen and V. J. Catalano, *Eur. J. Inorg. Chem.*, 2015, 5254–5261.
56 N. Tsukada, O. Tamura and Y. Inoue, *Organometallics*, 2002, **21**, 2521–2528.
57 M. Dahlen, E. H. Hollesen, M. Kehry, M. T. Gamer, S. Lebedkin, D. Schooss, M. M. Kappes, W. Klopper and P. W. Roesky, *Angew. Chem., Int. Ed.*, 2021, **60**, 23365–23372.
58 M. Dahlen, M. Kehry, S. Lebedkin, M. M. Kappes, W. Klopper and P. W. Roesky, *Dalton Trans.*, 2021, **50**, 13412–13420.
59 H. Schmidbaur and A. Schier, *Chem. Soc. Rev.*, 2012, **41**, 370–412.
60 G. A. Bowmaker, Effendy, S. Marfuah, B. W. Skelton and A. H. White, *Inorg. Chim. Acta*, 2005, **358**, 4371–4388.
61 M. T. Dau, J. R. Shakirova, A. J. Karttunen, E. V. Grachova, S. P. Tunik, A. S. Melnikov, T. A. Pakkanen and I. O. Koshevoy, *Inorg. Chem.*, 2014, **53**, 4705–4715.
62 P. Ai, A. A. Danopoulos, P. Braunstein and K. Y. Monakhov, *Chem. Commun.*, 2014, **50**, 103–105.
63 F. A. Cotton, X. Feng, M. Matusz and R. Poli, *J. Am. Chem. Soc.*, 1988, **110**, 7077–7083.
64 A. C. Lane, M. V. Vollmer, C. H. Laber, D. Y. Melgarejo, G. M. Chiarella, J. P. Fackler, X. Yang, G. A. Baker and J. R. Walensky, *Inorg. Chem.*, 2014, **53**, 11357–11366.
65 H. E. Abdou, A. A. Mohamed and J. P. Fackler, *Inorg. Chem.*, 2005, **44**, 166–168.
66 D. Fenske, G. Baum, A. Zinn and K. Dehnicke, *Z. Naturforsch., B: J. Chem. Sci.*, 1990, **45**, 1273–1278.
67 F. H. Allen, O. Kennard, D. G. Watson, L. Brammer, A. G. Orpen and R. Taylor, *J. Chem. Soc., Perkin Trans. 2*, 1987, S1–S19.
68 M. Dahlen, T. P. Seifert, S. Lebedkin, M. T. Gamer, M. M. Kappes and P. W. Roesky, *Chem. Commun.*, 2021, **57**, 13146–13149.
69 E. Hartmann and J. Strähle, *Z. Naturforsch., B: J. Chem. Sci.*, 1989, **44b**, 1–4.
70 P. N. Bartlett, F. Cheng, D. A. Cook, A. L. Hector, W. Levason, G. Reid and W. Zhang, *Inorg. Chim. Acta*, 2010, **363**, 1048–1051.
71 M. Stollenz, *Chem. – Eur. J.*, 2019, **25**, 4274–4298.
72 H. de la Riva, M. Nieuwhuyzen, C. Mendicute Fierro, P. R. Raithby, L. Male and M. C. Lagunas, *Inorg. Chem.*, 2006, **45**, 1418–1420.
73 M. Gil-Moles, M. C. Gimeno, J. M. López-de-Luzuriaga, M. Monge, M. E. Olmos and D. Pascual, *Inorg. Chem.*, 2017, **56**, 9281–9290.
74 O. Crespo, E. J. Fernández, M. Gil, M. Concepción Gimeno, P. G. Jones, A. Laguna, J. M. López-De-Luzuriaga and M. Elena Olmos, *J. Chem. Soc., Dalton Trans.*, 2002, 1319–1326.
75 T. P. Seifert, S. Bestgen, T. J. Feuerstein, S. Lebedkin, F. Krämer, C. Fengler, M. T. Gamer, M. M. Kappes and P. W. Roesky, *Dalton Trans.*, 2019, **48**, 15427–15434.
76 T. M. Dau, B. D. Asamoah, A. Belyaev, G. Chakkaradhari, P. Hirva, J. Jänis, E. V. Grachova, S. P. Tunik and I. O. Koshevoy, *Dalton Trans.*, 2016, **45**, 14160–14173.
77 Y. Takino, N. Yoshinari, T. Kawamoto and T. Konno, *Chem. Lett.*, 2012, **41**, 834–836.
78 D. J. Nielsen, K. J. Cavell, M. S. Viciu, S. P. Nolan, B. W. Skelton and A. H. White, *J. Organomet. Chem.*, 2005, **690**, 6133–6142.
79 M. Bierenstiel and E. D. Cross, *Coord. Chem. Rev.*, 2011, **255**, 574–590.